Journal of Building Engineering 76 (2023) 107406

Contents lists available at ScienceDirect

Journal of Building Engineering

journal homepage: www.elsevier.com/locate/jobe

Serviceability parameters and social sustainability assessment of flax fabric reinforced lime-based drywall interior panels

Ali Rakhsh Mahpour [a], Payam Sadrolodabaee [b], Mònica Ardanuy [c,*], Laia Haurie [a], Ana M. Lacasta [a], Joan R. Rosell [a], Josep Claramunt [d]

[a] Department of Architectural Technology, Universitat Politècnica de Catalunya (UPC), Barcelona, Spain
[b] Department of Civil and Environmental Engineering, Universitat Politècnica de Catalunya (UPC), Barcelona, Spain
[c] Department of Materials Science and Engineering, Universitat Politècnica de Catalunya (UPC), Barcelona, Spain
[d] Department of Agri-Food Engineering and Biotechnology, Universitat Politècnica de Catalunya (UPC), Barcelona, Spain

ARTICLE INFO

Keywords:
Acoustic behavior
Carbon uptake
Fiber-reinforced lime panels
Fire and thermal behavior
Flax fibers
Serviceability
Sustainability
MIVES

ABSTRACT

In the search of more environmentally-friendly construction materials, the use of natural-based fibers has gained much attention as reinforcement in the inorganic-based matrix. In this paper, the nonwoven flax fabric reinforced lime composites are created using a dewatering technique, and the serviceability parameters –thermal conductivity, sound absorption coefficient, and residual flexural resistance after exposure to elevated temperature– are determined experimentally. The tests are carried out on two different lime composites prepared under two distinct curing regimens, i.e., accelerated carbonation in a CO_2 chamber and natural carbonation in laboratory conditions, to evaluate the effect of forced carbonation. In addition, the experimental results of the serviceability parameters are included in the MIVES model (*Integrated Value Model for Sustainability Assessment*) to evaluate the social sustainability of the developed material as an interior drywall panel. MIVES, a type of multi-criteria decision-making method, is based on the value function concept and seminars with experts. According to the results of experimental tests, the accelerated cured sample has higher thermal conductivity (~4 times) and lower sound absorption coefficients (~20%) than the naturally cured one. Nonetheless, the flexural performance of the former is 50% (at room temperature) and 100% (at elevated temperature) better. As for the social sustainability index assessed by the MIVES-based multi-objective approach, it ranges between 0.65 and 0.75 (out of 1.0) for both lime composite panels, at least 20% higher than the control lime panel with no reinforcement. The sustainability model designed for this research can be used for assessing the social sustainability performance of other materials although the weights assigned by the experts could be adapted to reflect the perceptions and local preferences.

1. Introduction

Sustainable construction may play a crucial role in sustainable development goals. The building sector has a variety of negative effects on the environment during distinct phases, including material production, on-site building, the usage phase, and demolition [1, 2]. Therefore, this sector is responsible for over 35% of the European Union's total carbon footprint, 40% of its final energy

* Corresponding author.
E-mail addresses: ali.rakhsh@upc.edu (A.R. Mahpour), payam.sadrolodabaee@upc.edu (P. Sadrolodabaee), monica.ardanuy@upc.edu (M. Ardanuy), laia.haurie@upc.edu (L. Haurie), ana.maria.lacasta@upc.edu (A.M. Lacasta), joan.ramon.rosell@upc.edu (J.R. Rosell), josep.claramunt@upc.edu (J. Claramunt).

https://doi.org/10.1016/j.jobe.2023.107406
Received 13 May 2023; Received in revised form 7 July 2023; Accepted 19 July 2023
Available online 21 July 2023

consumption, and approximately 45% of its total waste generation [3]. For this reason, innovations aimed at improving the energy efficiency of construction elements and relying on more environmentally-friendly materials are of practical importance [4]. Within this context, internal walls, as essential construction elements, may improve energy efficiency and sustainability. While traditional brick walls are still being used in many developing countries, a new type of internal wall known as interior panels are receiving increasing interest.

Although gypsum-based interior panels are used mainly in many regions as drywall, they have certain disadvantages, including poor water resistance, high susceptibility to mold and mildew growth in humid climates, and low thermal insulation, among others [5]. Thus, internal boards made of other inorganic matrices such as lime or cement could serve as a promising alternative, especially when reinforced with sustainable fibers such as recycled or natural-based ones. Indeed, it is widely believed that adding fibers to mineral matrices could enhance certain properties of these materials, including toughness, energy absorption capacity, post-cracking residual strength, and crack control [6–11]. In general, the use of natural-based reinforcement offers a promising solution of low-cost, non-toxic, and eco-friendly materials [6,12]. According to *Dicker* et al. [13], fiber/textile-reinforced mortars (FRM/TRM) containing incorporated synthetic fibers consumed approximately five times more energy than their counterparts that were reinforced with plant fibers.

Over recent decades, many studies have been carried out on different cement-based composites reinforced with distinct types of natural reinforcement –short fibers, long fibers, or textiles [14–16]. However, research on lime-based composites is scarce and limited, even though it may offer an interesting option, especially for the conservation and restoration of archaeological sites and historic buildings, thanks to their physical, chemical, and mechanical compatibility with traditional building materials [17]. Indeed, certain properties of lime materials (mortars or pastes) such as moderate mechanical resistance, high durability, and good water vapor permeability have attracted the attention of researchers and engineers [18,19]. Furthermore, lime mortars appear to be more eco-friendly than cement since their hardening process is accompanied by the uptaking and capturing of CO_2. Moreover, lime production occurs at lower temperatures than cement clinker, resulting in a lower release of CO_2. Nonetheless, its extremely slow carbonation and hardening, leading to low strength at early ages, presents a major challenge. In fact, significant portlandite carbonation –and hence, the stable characteristics– may require months of curing, which is incompatible with the rapid construction needs of today's sector.

An accelerated carbonation process (CO_2 curing) using carbon incubators is one of the solutions offered to overcome the aforementioned challenge. The efficiency of this curing system depends on CO_2 concentration and pressure, carbonation time, relative humidity and temperature, as well as the composition of the lime mortar and its porosity [20,21]. *Ergenc* et al. [22] reported that CO_2 curing had noticeable effects on lime mortars by advancing calcite precipitation and therefore, offering early improvements on various properties as compared to those cured in a laboratory setting at ambient temperatures. *Cultrone* et al. [23] concluded that curing for 8 days at a high CO_2 concentration (0.7% CO_2 by volume) could promote a fast carbonation process to convert portlandite to 90 wt% calcite. However, the same level of conversion of $Ca(OH)_2$ to $CaCO_3$ took approximately 6 months using natural curing conditions. Similarly, *Dehilly* et al. [24] found that the carbonation reaction process was at least two times faster in a carbonic atmosphere than in low CO_2 conditions. *Silva* et al. [25] reported that lime mortars cured in a CO_2-rich environment (5% CO_2 by volume) carbonated faster and could reach a high degree of carbonation after only 7 days, with up to 98% of the portlandite converted to calcite. However, samples cured naturally in atmospheric concentration (0.05% CO_2 by volume) barely reached 70% of portlandite conversion into calcite, even after 6 months. In fact, advanced carbonation may occur through the exposure of the lime mortars to excessive CO_2 amounts, since the carbonation reaction is based on the diffusion (through open pores) and dissolution of CO_2 in capillary pore water, followed by the conversion of portlandite into calcite [26]. The gradual precipitation of calcium carbonate leads to the formation of a densely interconnected microstructure, with the material progressively strengthening over time [27].

As for the use of natural-based textile reinforcement in lime, several studies have reported the incorporation of woven fabrics. *Ferrara* et al. [28,29] studied the tensile behavior of hydraulic-lime mortar reinforced with flax woven fabrics and concluded that two-layer treated textiles (impregnated and coated with the polymeric substance) had optimized performance. Another study [30] examined the mechanical behavior of laminated natural TRM containing impregnated flax textile through the addition of short hornified curauá fibers within the lime matrix. These studies revealed that the lime TRM including vegetable fabric demonstrated strain-hardening behavior under the tensile load, presenting the typical tri-phase stress-strain curve, i.e., elastic linear phase, crack development stage, and progressive damage until failure. To the best of our knowledge, however, no prior studies have used nonwoven-type natural fabrics as reinforcement for lime composites.

As for the thermal and acoustic insulation performance of the lime composites, there are few studies available in the literature whereas, to the best of our knowledge, no notable studies have been found on the behavior of lime composites exposed to elevated temperature. *Quintaliani* et al. [31] investigated the thermal and acoustic performance of natural hydraulic lime mortars reinforced with 10% of various vegetal fibers in two distinct forms, as-found and ground. Based on their results, the thermal conductivity of the lime composites was reduced by 10% (as-found size) or 20% (ground size) than the control mortar (without any reinforcement). Nonetheless, the addition of those fibers could hardly affect the sound insulation properties. In another study, *Kinnane* et al. [32] examined the acoustic behavior of hemp-lime concrete made from various binders including hydrated lime (CL90), hydraulic lime (NHL 3.5), cement (type-I), and different pozzolans (metakaolin and ground granulated blast furnace slag). The results revealed that the composite continuing hydrated lime-pozzolan had a higher sound absorption coefficient than those incorporating cement or hydraulic lime, due to the lower density of the lime-pozzolan concrete. Thus, the authors concluded that there was an inverse relationship between sound absorption and hydraulic binder content in the composite.

Prior studies performed by our group on the hydrated lime mortars examined the rheology and mechanical behavior of lime paste, as well as its possibility of penetrating a nonwoven natural flax fabric type [33,34]. According to the results of those studies, a blended

lime matrix with 20% metakaolin (MK) demonstrated the best performance, also improving the mortar's durability due to the formation of denser hydrated products such as C–S–H gel through pozzolanic reaction [35,36]. In this study, a similar lime matrix was used to fabricate the laminated composite reinforced with nonwoven flax fabric, which has rarely been considered in the literature. To specify the potential application of the developed lime composite, either as a strengthening solution for masonry or an internal/-external panel, the technical parameters related to thermal and acoustic performances were investigated. In addition, post-fire behavior was evaluated based on residual flexural resistance after exposure to different temperatures (20 °C–950 °C). All of the mentioned technical parameters, scarcely reported on for lime TRM composites in the literature, were evaluated for the composite plate cured in laboratory conditions and the one cured by forced carbonation, to also examine the effect of accelerated carbonation. Finally, the analyzed serviceability parameters were implemented in the MIVES model (*Integrated Value Model for Sustainability Assessment*) to evaluate the social sustainability index of the developed laminate composites as internal panels. Thus, the objectives of this research work are summarized as follows:

- Developing the flax nonwoven fabric reinforced lime panels under natural and accelerated carbonation;
- Characterizing the serviceability parameters of the lime panels including thermal and acoustic insulation as well as fire behavior through the experimental tests;
- Assessing the social sustainability index of the lime panels by implementing the experimental characterization through the MIVES-based multi-objective approach.

2. Methods

The proposed outline of this research work (see Fig. 1) was classified into two main categories: the experimental campaign and the sustainability model design, which are described in detail in the following sections.

2.1. Experimental program

2.1.1. Materials and composite fabrication

According to our previous study [33], the optimum lime matrix for the production of the composite consisted of slaked lime mixed with 20% metakaolin (MK) with an initial water-to-binder ratio (w/b) of 1.0. Powdered slaked lime (CL90 with 90% portlandite) and MK (with a specific weight of 2.5 g/cm^3, 40% alumina, and 54% silica) –supplied by *Dcal By Ciaries, SLU (Olesa de Bonesvalls, Barcelona, Spain)* and *Arcillas Refractarias ARCIRESA, SA (Gijón, Asturias, Spain)*, respectively– were used to produce the paste. All of the chemical and physical properties of CL90 and MK have been reported elsewhere [33]. No aggregate was added to the paste since this could inhibit mortar penetration into the nonwoven flax [37].

Flax fibers (60 mm length) provided by *Institut Wlokien Naturalnych (Poland)* were used to create a light nonwoven fabric reinforcement through a needle punching process, described in detail elsewhere [38]. The produced fabrics were subjected to four wet-dry cycles of oven drying for 8 h at 60 °C followed by a 16-hr water immersion at 20 °C to improve the dimensional stability and durability of the vegetable fibers in the alkalinity environment of the matrix, thereby improving adherence between fiber and matrix [39]. The final fabric (Fig. 2a), approximately 1 mm thick, had an areal weight of 190 g/m^2 and a tensile rupture load of 3.70 ± 1.41 N/g (normalized per weight) as reported in a previous study [40].

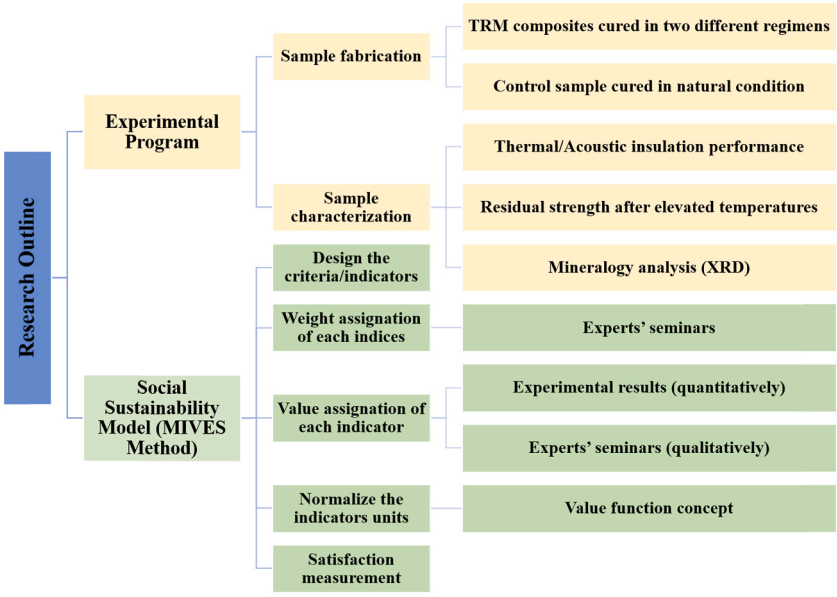

Fig. 1. Research workflow diagram.

For composite preparation, a method based on the adequate penetration and impregnation of the lime paste into the nonwoven fabrics by hand lay-up and stacking techniques was used. The production of the composite laminated plate was carried out in a specific drilled mold having internal dimensions of 300 mm × 300 mm × 10 mm (Fig. 2b). Produced laminates had six nonwoven layers with a fiber weight fraction of 9%, selected as the optimum layer number based on a previous study [40]. They were impregnated with cross-oriented lime paste (Fig. 2c). Dewatering treatment –including the elimination of excess water by vacuuming and compressing the mold for 24 h under 3.3 MPa pressure– was carried out to remove excess water. Two plates, i.e, composite and control (without fiber) were cured naturally for 28 days at ambient air in a lab environment while one composite plate underwent accelerated curing for 7 days in a CO_2 incubator by injection of CO_2 gas until reaching a pressure of 0.20 MPa (2 atm). The control sample without reinforcement was used to assess the effect of the addition of the fibers.

Table 1 shows the nomenclature and mix-design of the plates. The mass of the sample after accelerated carbonation varied marginally since, on the one hand, the mass may decrease as the paste dried rapidly due to evaporation of capillary pore water induced by the heat released during the exothermic carbonation reaction [22]; and, on the other hand, the mass may increase due to the transformation of portlandite into calcite (with a relative molecular mass of 74.0 and 100.0, respectively) [41].

2.1.2. Thermal conductivity test

The thermal conductivity coefficient of the plates was determined through the transient line-source method, using Quickline-30 equipment from Anter Corporation, according to ASTM D5930 [42]. Briefly, the device analyzed the response of the material to heat flow variations induced by a superficial probe. Given the low thickness of the plate (~10 mm), two overlapping specimens (100 × 100 × 10 mm) were used for the measurement to avoid any possible errors by the device. A similar method has been reported to calculate the thermal conductivity of cementitious materials in other studies [4,43–45].

2.1.3. Acoustic absorption test

Cylindrical specimens with diameter and height of 50 and 10 mm, respectively, were used to assess the acoustic properties of the samples, namely the sound absorption coefficient, as shown in Fig. 3a. Measurements were performed in an impedance tube according to the UNE-EN ISO 10534-2 standard [46], as described in detail elsewhere [47]. In short, the principle is based on transfer function measurements between two microphones. The sound source was connected to one end of the tube, and the sample was placed at the other end. Acoustic pressures were measured at two tube positions near the sample using two microphones mounted 50 mm between them. The source generated a random signal from which the complex acoustic transfer function was determined for frequencies in the 500–3150 Hz range.

2.1.4. Fire tests

2.1.4.1. Epiradiator test. A fire reaction test was performed using an epiradiator described in the standard UNE 23725-90 [48] to evaluate the impact of the addition of nonwoven fabric on the composite's fire behavior. Specimens measuring 100 × 100 mm^2 were placed on a metallic grid 30 mm below a heating source of 500 W, which implied a heat flux of 3 W/cm^2, for 5 min. If the sample ignites during the 5 min of the test, the radiator must be removed and returned once the flames have been extinguished. Parameters considered in this test include the number of ignitions (N∘), the time when the first ignition occurs (t_0), the average time of flame persistence, and the sample's weight loss during the test.

2.1.4.2. Post-fire residual flexural resistance. The effect of exposure to high temperatures (250–950 °C) on the properties of the plates was evaluated using a small-scale oven (Hobersal JM3-15 oven), as shown in Fig. 3b. Samples of 150 mm × 50 mm were placed in the oven and temperature gradients were changed as seen in Fig. 4.

Three specimens (150 mm × 50 mm) were tested under a 3-point bending configuration to examine the flexural behavior of the materials at different temperatures: 20 °C, 250 °C, 450 °C, and 950 °C (Fig. 3c). The crosshead speed of *TA.XT plus texturometer*, equipped with a load cell of 0.5 KN, was 6 mm/min while the spacing between supports was 120 mm. The limit of proportionality (LOP) as the matrix's threshold strength, modulus of rupture (MOR) as the maximum flexural strength of the composite, flexural modulus (MOE), and toughness index (I_G) were calculated using the approach described in the previous studies [12,43]. Finally, the flexural strength (MOR) loss rate after exposure to high temperatures was calculated.

2.1.5. Mineralogy identification

After the flexural tests, the samples were ground into fine powders and subjected to X-ray diffraction (XRD) analysis for mineralogical characterization. This was performed using a *Bruker AXS D8 Discover powder diffractometer* using a 15° to 65° 2θ explored area

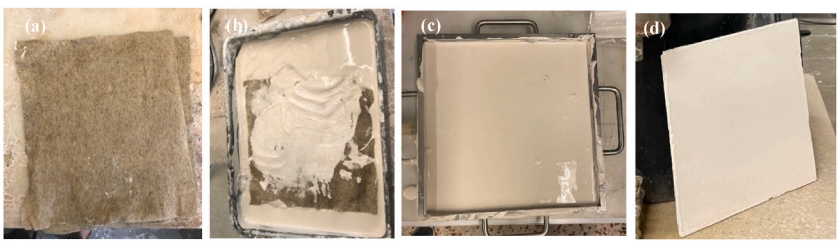

Fig. 2. Lime panel production: a) nonwoven fabric; b) impregnation of the lime paste into the nonwoven fabrics; c) casting in the mold; d) lime boards.

Table 1
Mix proportions of the composite plates.

Sample	Lime [gr]	MK [gr]	Water [gr]	$(w/b)_{final}$	Final apparent density [g/cm^3]
AC: accelerated carbonated composite	800	200	1000	0.55	1.39
NC: naturally carbonated composite	800	200	1000	0.50	1.22
Control: naturally carbonated sample without fiber	1200	300	1500	0.55	1.35

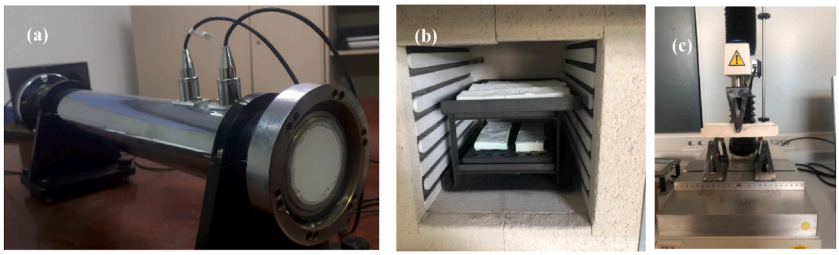

Fig. 3. Experimental tests setup: a) Acoustic test; b) small-scale oven; c) flexural test.

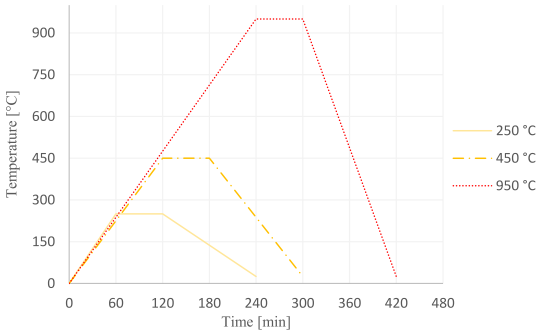

Fig. 4. Temperature evolution for the exposed samples in the small-scale oven.

and a speed of 0.02 2θ/s with CuKα radiation of 1.5418. Using the Match! V3.15 software and RIR (reference intensity ratios) values, the generated patterns were subjected to semi-quantitative analysis to identify the relative quantities of the mineral phases found in the samples.

2.2. Sustainability model design

To facilitate the selection of sustainable and efficient building materials in the construction industry, sustainability assessment of specific building elements should be further investigated by considering certain pillars of sustainability: economic, environmental, and social. Although most available literature has focused solely on environmental sustainability performance [49–51], in this study, social performance was analyzed through the MIVES model by implementing the obtained experimental results of the serviceability parameters.

MIVES, *Modelo Integrado de Valor para una Evaluación Sostenible* (Spanish) which means *Integrated Value Model for Sustainability Assessment*, is a type of multi-criteria decision-making (MCDM) approach that incorporates both qualitative and quantitative indices (with diverse units and scales) to achieve a final sustainability index (SI). Among the various MCDM methods (e.g., BREEAM, LEED, DGNB, and CEEQUAL), MIVES has proven to provide a representative and meaningful quantification of sustainability in different areas of civil engineering [52]; including energy (e.g., wind towers [53] and solar energy [54]), urban (e.g., post-disaster in urban areas [55, 56] and sewerage pipe system [57]), buildings (e.g., prefabricate [58] and industrial buildings [59]), building elements (e.g., steel fibers [60] and facades [61]), infrastructures (e.g., railway [62], tunnels [63] and bridges [64]), among others.

MIVES methodology was comprehensively explained in previous mention studies. To summarize, as shown in Fig. 1, this multi-objective method consists of five main steps: a) identifying the indices of the decision-making process including requirements, criteria, and indicators; b) assigning weights for each index; c) estimating the value of each indicator based on its unit; d) normalizing the value of each indicator to dimensionless value by applying value function concept; e) measuring the satisfaction value index of each index. To accomplish the mentioned steps, expert seminars may be applied wherever needed.

In the present study, only one requirement, i.e., the social performance of the prefabricated lime board as an interior panel was assessed. To identify the criteria/indicators for this requirement, the recently proposed MIVES model by the authors for assessing the

sustainability of the façade cladding panels of residential buildings in Barcelona [65,66] was used (with small modification). According to the modified proposed model, see Table 2, five indicators (the most representative, independent, and quantifiable) within the three criteria were selected for the social sustainability requirement, aiming to improve the quality of users' life as well as that of third parties. The *Comfort* (C_1) criterion consisted of two indicators: *Thermal* (I_1) and *Acoustic performances* of the internal panels (I_2). I_1 was evaluated by the thermal conductivity of panels and I_2 was assessed by the noise reduction coefficient (NRC) which, in turn, was calculated from the sound absorption coefficient. The *Safety* (C_2) criterion included two indicators of *Fire* (I_3) and *Jobsite Risks* (I_4). The former (I_3) calculated the flexural strength loss rate of the panels after exposure to high temperatures. The latter (I_4) showed the probability of accidents for labors or the public during the manufacturing and building phases. I_4 was qualitatively rated on a measurable scale of 1–5 through seminars with experts, considering the complexity and danger of assembling/installing [67]. Finally, the *Aesthetic* (C_3) criterion including the *Visual quality* indicator (I_5) evaluated the architectural style of the panel (qualitatively through expert seminars) on a measurable scale of 1–10, considering form, color, texture, and size [44]. Thus, the indicators' values of $I_I - I_3$ were quantitatively assessed using the experimental results, whereas the others ($I_4 - I_5$) were qualitatively evaluated through seminars with 10 experts (including architects, civil/building engineers, and researchers from UPC-BarcelonaTECH) who have already experiences with MIVES method.

After identifying the parameters of the decision-making process, the indices (indicators and criteria) were weighted and prioritized by the same experts using the simplified analytical hierarchy process (AHP-based) through a questionnaire survey. In other words, the indices of each group (C_1–C_3; I_1–I_2; and I_3–I_4) were compared pairwise to be weighted and prioritized. In the next step, after quantifying each indicator (X_1-X_5) and knowing the weights of indices, the value function concept was used to transform the calculated values of the indicators (X_1-X_5) into a dimensionless value ranging from 0.0 to 1.0. Indeed, defining the value functions adds homogeneity to the variables by transforming them into common, non-dimensional units called satisfaction values. The satisfaction value for each indicator (*Vi*) represents the preference for a certain alternative and varies between the minimum ($V_{min} = 0$) and maximum ($V_{max} = 1$) satisfaction levels. Thus, through this normalization of the indicators' units, the satisfaction value of the stakeholders and users was measured, ranging from 0.0 to 1.0. A value of 1.0 demonstrates the maximum degree of sustainability satisfaction, associated with the X_{max}, while a value of 0.0 suggests minimum satisfaction, corresponding to the X_{min} (see Fig. 5). X_{max} and X_{min} for each indicator were defined according to past projects, literature reviews, and the value produced by the different alternatives (see sources in Table 2).

The value function for each indicator -to connect the two coordinates of (X_{min},0.0) and (X_{max},1.0)- has a specific shape and tendency selected based on the MIVES model definition [68] and the experts' seminars. The tendency of the value function could be increasing (I) or decreasing (D), while the shape could be selected among concave (C_v), convex (C_x), linear (L), or S-shaped (S), as shown in Fig. 5. Thus, the satisfaction value of each indicator (V_1–V_5) was estimated based on Eqs. (1) and (2) (or roughly from the value function diagram), and then, the satisfaction level of the three criteria and the social requirement was measured by considering the assigned weight. More detailed explanations of the MIVES approach and the guidelines for selecting the parameters have been reported in other referenced works [61,69,70].

$$V(i) = A + B \cdot \left[1 - e^{-k_i \cdot \left(\frac{|X_i - X_{min}|}{c_i} \right)^{P_i}} \right] \quad \text{Eq.1}$$

$$B = \left[1 - e^{k_i \cdot \left(\frac{|X_{max} - X_{min}|}{c_i} \right)^{P_i}} \right]^{-1} \quad \text{Eq.2}$$

Where

V_i: the indicator's satisfaction value;
A: response value of X_{min} (mostly A = 0);
B: a factor that keeps the function in the range of 0.0–1.0;
X_i: an indicator that generates the value V_i;
X_{min}: point with the lowest satisfaction;
X_{max}: point with the highest satisfaction;
P_i: shape factor, which will be $P_i < 1$ (if the function curve is concave), $P_i > 1$ (if the function curve is convex), or $P_i = 1$ (if the function curve is linear)

Table 2
Indicators and Criteria for the social sustainability assessment.

Requirement	Criteria	Indicators	Units	Sources
Social	C_1.Comfort (50%)	I_1. Thermal performance (50%)	W/(mK)	Experimental results; Scientific literature [31,43,44,71–73]:
		I_2. Acoustic performance (50%)	points	Experimental results; Scientific literature [31,65,72,74–76]:
	C_2.Safety (40%)	I_3. Fire risk (60%)	%	Experimental results; Scientific literature [43,65,77–79]:
		I_4. Jobsite risk (40%)	Points	Seminars with experts; Scientific literature [67]:
	C_3. Aesthetic (10%)	I_5. Visual quality (100%)	Points	Seminars with experts; Scientific literature [44,67]:

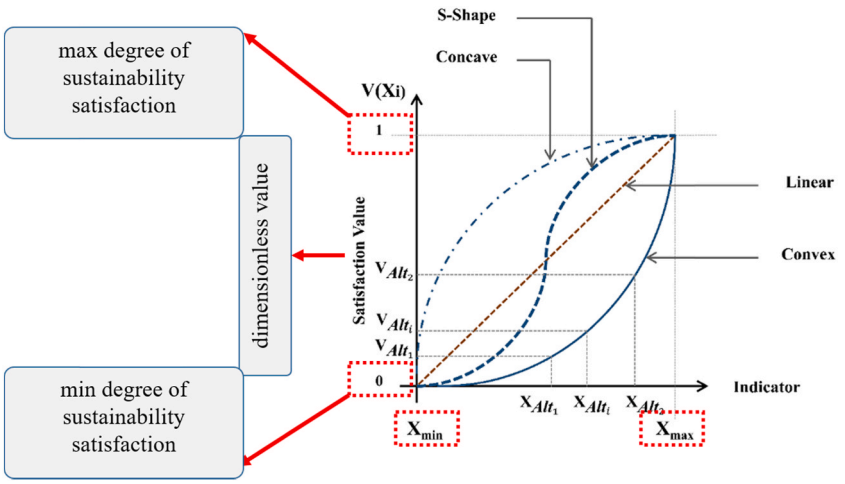

Fig. 5. Value function concept based on the MIVES model.

C_i: factor that is used for the inflection point in curves with $P_i > 1$.
K_i: factor that describes the response value to C_i;

3. Results and discussion

3.1. Thermal conductivity

As shown in Table 3, the ACC sample had a thermal conductivity that was four times greater than that of the NCC, suggesting that the accelerated lime carbonation worsens the material's thermal behavior. Indeed, porosity decreased by developing the carbonation since the solid volume increased with the conversion of CH into calcite crystals (see Table 1) [41,80]. Therefore, it was reported that the porosity reduction of the lime mortar after 180 days of chamber-curing was 67% while for the naturally-curing one, it was only 24% [81]. Nonetheless, both composites showed high thermal insulation performance as the incorporated vegetable fibers could increase porosity and decrease thermal conductivity [31]. It is evident that the control sample without fiber had 3 times the thermal conductivity as the one with fiber under the same conditions (NC). Similarly, the thermal conductivity of inorganic matrices reinforced with natural-based fibers ranged from 0.2 to 0.9 W/(mK), for instances wood-gypsum boards, nonwoven fabric cement boards, and vegetal lime mortars varied in the range of 0.2–0.7 [73], 0.65–0.86 [43,44], and 0.52–0.71 [31], respectively. Nonetheless, this parameter for some types of concrete and cement panels may reach 2 W/(mK) [71]. The values reported in Table 3 were used for indicator I_1 in the sustainability model.

3.2. Acoustic absorption behavior

The sound absorption coefficient of the lime samples is shown in Fig. 6. The maximum values for the Control, NC, and AC samples were 0.11 (at a frequency of approximately 500 Hz), 0.28 (at a frequency of approximately 3150 Hz), and 0.24 (at a frequency of approximately 1600 Hz), respectively. Thus, accelerated carbonation decreased the acoustic absorption of the flax/lime composite by up to 15% due to the denser structure. Like thermal behavior, acoustic performance depends on the porosity of the materials, and absorption may be improved by increasing the porosity. This may be achieved in distinct ways, such as incorporating lightweight aggregates, foams, or vegetal fibers [31,76]. The acoustic absorption coefficient of the Control was 60% less than that of the NC composite. Similarly, for lime plaster without fiber, this value was reported to be approximately 0.06 [82]. For indicator I_2 in the MIVES model, the noise reduction coefficient (NRC) was calculated. This is the average value of sound absorption coefficients at frequencies of 500, 1000, and 2000 Hz. The values of this parameter for the Control, NC, and AC specimens were approximately 0.08, 0.20, and 0.15, respectively. The typical value of the absorption coefficient and NRC for the mineral composite panels was less than 0.5. For instance, the maximum acoustic absorption coefficients for hydraulic lime panels with textile waste fibers, hybrid nonwoven fabric cement boards, and cement-wood boards were reported to be approximately 0.3, 0.26, and 0.41, respectively [44,82]. Similarly, the sound absorption average for lime mortars including different vegetal fibers was in the range of 0.24–0.38 [31]. Furthermore, the NRC for several hemp lime mortars and concretes were reported to be less than 0.5 [32,76].

Table 3
Values of thermal conductivity for all samples.

Sample	Thermal Conductivity [W/(mK)]
AC	0.42 ± 0.054
NC	0.10 ± 0.019
Control	0.31 ± 0.015

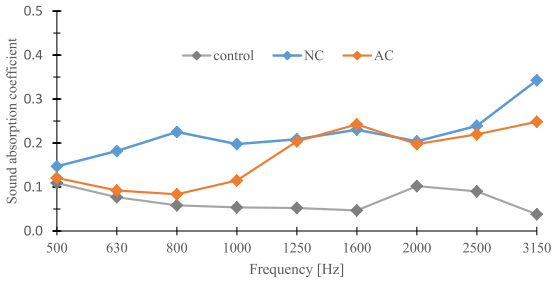

Fig. 6. Sound absorption coefficient spectra of lime panels.

3.3. Fire behavior

3.3.1. Epiradiator test

During the epiradiator test, upon reaching a temperature of 420 °C for 5 min, a small amount of unclear and semi-visible smoke and flames were detected at the last minute of the test. They immediately vanished when removing the heat source. Fig. 7 shows the unexposed and exposed (to the radiation) surfaces of the NC sample. The exposed surface became dark and cracks were observed on it, although there was no significant detachment of the material given the remaining bridging effect of the fibers [83]. The average weight loss of the irradiated samples was 18.6%, due to water evaporation, dehydration, and the conversion of lime compounds into oxides. Similarly, changes in appearance and mass loss for cement-based composites subjected to high temperatures were reported by other authors [84]. *Zhang* et al. [77] reported a 17.9% mass loss of cement composite reinforced with polyvinyl alcohol (PVA) short fibers after exposure to 400 °C, whereas *Sadrolodabaee* et al. [65] and *Gonzalez* et al. [43] reported a mass reduction of 15.6% (for the cement TRM reinforced with recycled textile waste fabric) and 13.9% (for the calcium aluminate cement TRM reinforced with flax fabric), respectively.

3.3.2. Post-fire residual flexural resistance

Fig. 8 shows images of the samples after exposure to different elevated temperatures. At 250°C, both AC and NC samples remained with virtually no major visible cracks. At 450°C, the AC sample revealed several superficial and evenly distributed fissures while the NC had more separated and thicker cracks due to the water loss caused by sample drying and dehydration. Nonetheless, at 950°C, the NC broke down completely while the AC maintained its integrity, although having several deep and thick cracks. Thus, as the temperature rose, the samples developed a cracking pattern with more separated and thicker fissures. Furthermore, spalling of the matrix at elevated temperatures did not occur since the lime matrices are inherently porous (as compared to the dense Portland cement) and the addition of fibers caused the pressure to release even more slowly [77,79]. As *Zhang* et al. [77] reported, after exposure to 600°C, the number of microcracks in the cementitious composite samples increased significantly while the microstructure loosened. In general, the NC samples' microstructure became loose faster after being subjected to high temperatures due to the incomplete transformation of CH to calcite, whereas the AC sample displayed a denser microstructure.

The effect of high temperatures on the flexural performance of the composites is shown in Fig. 9. Table 4 summarizes the average mechanical parameter values. In Fig. 8, it can be seen that the composites that were not exposed to high temperatures (20 °C) displayed typical flexural-hardening behavior, i.e., the curves began with the linear elastic stage until the first fracture appeared in the matrix (LOP); then, the crack propagation zone began to display a sawtooth wave pattern in which both the matrix and the fibers contributed to the composite's strength; and finally, the post-cracking stage occurred with no new cracks appearing and with the existing ones becoming deeper until the reinforcement failure and ultimate fracture of the sample. The flexural strength of the presented lime composite board was significantly higher than that of other counterparts such as gypsum composites with cork (0.10–0.96 MPa) [85], polypropylene fiber-reinforced aerial lime mortars (0.2–1.4 MPa) [86], hydraulic lime composites with textile fiber waste (0.12–0.98

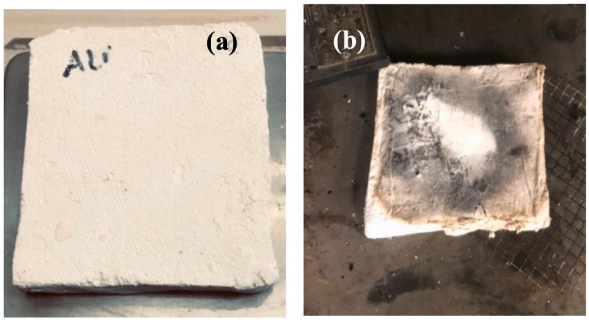

Fig. 7. Epiradiator test: a) unexposed surface of the NC sample to the heat source; b) exposed surface of the NC sample to the heat source after 5 min.

Fig. 8. Images of the composites after the small-scale fire test at different temperatures: a) AC-250, b) AC-450, c) AC-950, d) NC-250, e) NC-450, f) NC-950.

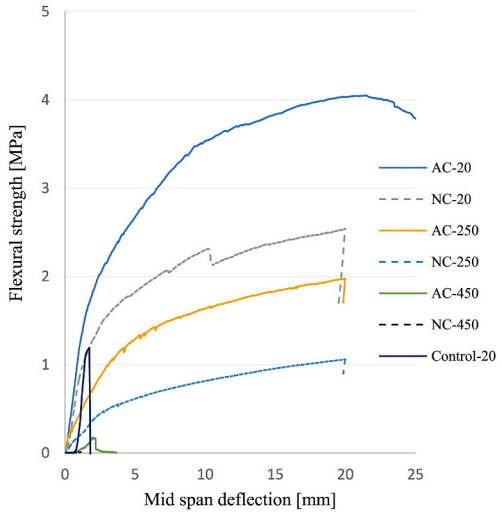

Fig. 9. Representative bending curves of samples exposed to different temperatures.

MPa) [82] or hydraulic lime composites with 1–2% glass/basalt fibers (1.5–2.4 MPa) [87]. However, the Control sample at 20 °C displayed brittle performance since there was no reinforcement to contribute to post-cracking. In fact, the incorporation of nonwoven flax layers increased maximum bending strength by up to 150%.

After exposure to 250 °C, the first stage was similar to that of the unexposed composites, but with a lower slope (MOE) and LOP,

Table 4
Average values of mechanical parameters under bending test. Cov in (%).

CODE	LOP (MPa)	MOR (MPa)	MOR/LOP	MOE (GPa)	Toughness (KJ/m^2)
Control - 20oC	1.3 (23)	1.3 (16)	1.0	0.15 (25)	0.04 (19)
AC - 20oC	3.30 (23)	4.85 (14)	1.45	0.32 (17)	3.2 (10)
NC - 20oC	2.40 (30)	3.20 (18)	1.35	0.22 (16)	2.5 (18)
AC - 250oC	1.90 (10)	2.30 (35)	1.20	0.20 (34)	1.2 (12)
NC - 250oC	1.15 (17)	1.35 (36)	1.20	0.15 (18)	0.9 (14)
AC - 450oC	0.20 (15)	0.20 (42)	1.0	0.05 (28)	0.09 (20)
NC - 450oC	0.06 (29)	0.06 (19)	1.0	0.02 (39)	0.02 (15)

suggesting partial damage to the matrix. The second zone was accompanied by fewer cracks due to the fibers' damage, leading to lower energy absorption and toughness. Temperatures exceeding 450 °C led to brittle failure in composites, i.e., the fibers could not contribute effectively since they decomposed and lost their bond with the matrix. This behavior is comparable to that of inorganic matrices with no reinforcement (Control sample at 20 °C). Indeed, the cellulose and hemicellulose of flax fibers break down between 250 and 450 °C whereas lignin decomposes between 200 and 500 °C [88,89]. Finally, the NC-950 °C was shattered before beginning the test while the AC-950 °C and the Control-250 °C were broken during pre-loading. Thus, there were no records for them.

As seen in Tables 4 and in composites not exposed to high temperatures (both AC and NC at 20 °C), the reinforcing effect of the flax fibers permitted relatively high deformability, leading to an increase in toughness and post-cracking flexural strength (MOR/LOP > 1.3). After subjecting the samples to 250 °C, the matrix strength decreased by 40% due to the internal pores and microcracks produced by evaporated water. Nonetheless, the non-decomposed reinforcement displayed high effectiveness despite a reduction in strength (MOR/LOP ≈ 1.20). After exposure to 450 °C, the bending performance changed considerably, i.e., the fibers lost their effectiveness and the material behaved relatively brittle, similar to the Control sample at room temperature (MOR ≈ LOP). Indeed, as previously reported [77], under 400 °C, the fibers remained beneficial to the mechanical strength of the composite, while at higher temperatures, melted/decomposed fibers could create pores and channels, leading to a decreased sample strength. Thus, LOP and MOE decreased dramatically for both AC and NC samples (see Table 4) since the matrix was decomposed and severely degraded after exposure to elevated temperatures. Furthermore, the toughness decreased significantly since it depended mainly on the fiber pull-out mechanism. Finally, exposure to 950 °C led to overall matrix destruction.

As for the curing regimen, generally accelerated carbonation led to better mechanical performance than natural carbonation for the same temperature since the calcite products derived from the carbonization reaction existed more in CO_2-chamber-cured samples, thereby forming a relatively denser paste structure, which led to higher mechanical strength [18]. As for the flexural strength loss rate after exposure to high temperatures, this value for the AC and NC samples was 52% and 58% at 250 °C, and 95% and 98% at 450 °C, respectively. For the Control, the resistance loss was 100% at elevated temperatures. In the study by *Vejmelkova* et al. [78], flexural resistance of the hybrid PVA cement FRM subjected to 800 °C was reduced by 82.7% while this loss rate was 82.9% at 600 °C for PVA fiber-reinforced cement composite in Ref. [77]. Similarly, *Gonzalez* et al. [43] reported 48% (at 250 °C), 73% (at 450 °C), and 90% (at 950 °C) MOR reduction for the calcium aluminate cement composite reinforced with flax fabric while this loss rate was 99% at 950 °C for the cement composite reinforced with recycled textile waste fabric [65]. As for indicator I_3 in the sustainability model (fire risk), values at 250 °C were selected as the index for interior panels.

3.4. Mineralogy identification

Fig. 10 presents the XRD spectra for the AC and NC samples exposed at different temperatures between 20 °C and 950 °C. Typical

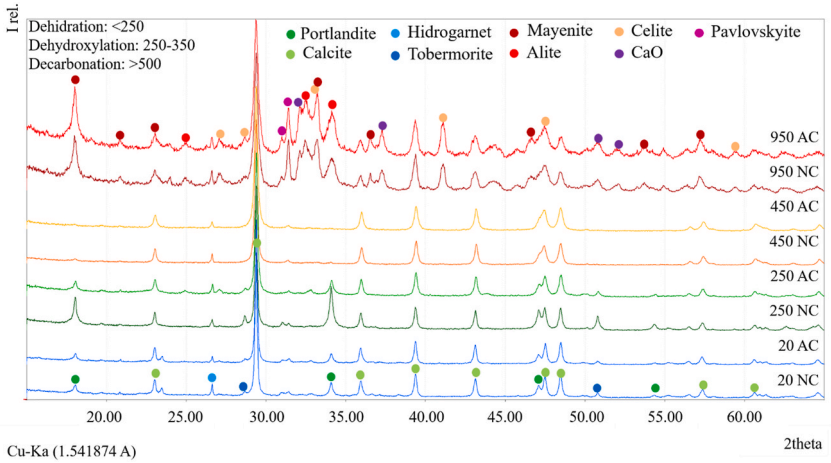

Fig. 10. *XRD sample* patterns.

minerals of lime, portlandite, and calcite were observed in the samples at 20 °C, with the latter being derived from the carbonation of the former. The incorporation of metakaolin as a pozzolanic substance led to the formation of a tobermorite-like C–S–H gel structure (from a combination of calcium and silicon), as well as a hydrogarnet-like structure from a combination of calcium and aluminum, both silicon and aluminum generated from metakaolin. The hydrogarnet could, in fact, be the stable phase of the initial formation of strälingite [90]. As for the different curing regimens at 20 °C, slightly more intense peaks of tobermorite and hydrogarnet were observed for the NC sample, due to the higher concentration of calcium from the portlandite. This concentration of portlandite would be lower in the case of the forced carbonated sample, resulting in a higher calcite concentration.

As for the samples at 250 °C, the NC sample displayed an increase in the portlandite peak, presumably due to greater precipitation of nanocrystalline $Ca(OH)_2$ retained in C–S–H, or the hydration of new CH crystals from existing CaO in the paste with steam as a consequence of the temperature increase [84,91,92]. Furthermore, a minor increase in the tobermorite peak was observed, caused by the increase in the speed of the pozzolanic reaction with the temperature. These observations in the NC sample most likely occurred at the beginning of the thermal ramp when the sample had yet to be dehydrated from the heat. On the other hand, this effect was not observed in the accelerated carbonate matrix due to the consolidation of calcium from the carbonation.

As for the samples corresponding to 450 °C, no significant differences were observed between the AC and NC samples. In both, only the peaks corresponding to the calcite that had not yet reached the temperature of decarbonization remained. Indeed, it was the only compound that did not degrade. Likewise, samples subjected to 950 °C did not display critical differences in terms of carbonation type. In both samples, new compounds appeared from the sintering of the previously decomposed compounds, from the combination of calcium, silicon, and aluminum ions (regardless of whether the calcium ion came from the dehydration of the CH or decarbonization of $CaCO_3$ at high temperature). Thus, compounds similar to those obtained in the manufacture of cement clinker appeared, such as alite, Celite, calcium oxide, or mayenite, as well as other highly crystalline compounds such as Pavlovskyite.

3.5. Sustainability analysis

The value functions and their related parameters for the five indicators can be found in Table 5. Three indicators with decreasing tendency are seen: I_1 with a convex shape, I_3 with a concave shape, and I_4 with a linear shape. On the other hand, two indicators display an increasing tendency, including I_2 (concave) and I_5 (linear). For example, Fig. 11 demonstrates the function shape (decreasing convex) of the I_1 where the satisfaction value of the *Thermal performance* decreases rapidly initially, with the increasing of thermal conductivity of the material.

Fig. 12 shows the satisfaction values of all indicators and criteria as well as the sustainability index (SI) of the social requirement for all three lime panels. To calculate the satisfaction levels of the criteria and the SI of social requirement, the final assigned weights (shown in percentage in Table 2) were employed. For instance, the two indicators of the *Comfort* criterion had the same weight (each had 50% with the same importance), thus the satisfaction value of C_1 will be equal to $0.5V_1+0.5V_2$. It is evident that the indicators of the NC composite panel varied in the range of 55–100%, the AC in the range of 43–74%, and the Control in the range of 0–74%. Indicator I_1 of the NC had the highest value of satisfaction (100%) of all the indices while indicator I_3 of the Control had the lowest value (0%). Several indices had values above 70%, which demonstrated very high sustainability levels, while the SI of the social requirement, according to the proposed weight, reached levels of 74%, 65%, and 45% for the NC, AC, and Control panels, respectively. Thus, the incorporation of flax nonwoven fabric could enhance the SI of the panel by 30% under natural carbonation.

The naturally-carbonated composite (NC) had a higher level of comfort satisfaction (i.e., better thermal and acoustic performance) than the AC and the Control, due to the higher porosity, as discussed previously in Sections 5.1 and 5.2. As for I_3, despite the fire vulnerability of the lime composite panel, especially the chamber-cured one, it was better than those of prefabricated fiber-reinforced polymer (FRP) composite panels [79], with the fiber cement boards offering better resistance as compared in Section 5.3. The lime panel without fiber (Control) was completely vulnerable to the high temperature, with a 0% satisfaction value. As for the I_4, the use of prefabricated panels as internal walls decreased the jobsite vulnerability for the workers since only assembly should be carried out on the site, as compared to certain more traditional construction systems such as brickwork. Finally, I_5 (and thus C_3) may be enhanced by taking some initiatives such as the production of larger panels or coated ones, although the developed panel could be used without any other special finishing.

Nonetheless, it should be noted that this sustainability model only considered the social requirement for the developed lime/flax panels mainly used in interior panel applications. To reach a more comprehensive conclusion, other pillars of sustainability including economic, environmental, and technical ones, should also be implemented. Furthermore, the indicators assigned in this model, although representative, could be modified/extended based on the location and function of the assumed building. For instance, the risk of natural disasters such as earthquakes may be added or substituted for other risks, such as that of fires. This is the case for our Barcelona case study since it is not situated in a seismic zone. Therefore, Occupational and Fire risks were selected. In other words, although the selected value functions and associated parameters may be taken as a reference for other panels, they should be updated and tailored to each unique situation according to the preferences of the stakeholders involved in the decision-making process.

4. Conclusions and perspectives

Research on fiber/textile-reinforced lime-based mortars is still scarce compared to that on cement-based ones. Likewise, studies on thermal, acoustic, fire, and sustainability properties of this type of material have been rarely reported. Therefore, this paper presented the experimental results from a study of the serviceability parameters of flax nonwoven fabric-reinforced lime composites cured in two different regimens: ambient air (NC) and accelerated chamber (AC). Furthermore, a control panel without fiber (under ambient conditions) was characterized. Finally, the social sustainability of the developed panels as an internal partition wall was assessed by

Table 5
Parameters *and values of each indicator for panel boards.*

Indicators	Units	Function Shape	X_{min}	X_{max}	C	K	P	$X_{i\text{-}AC}$	$X_{i\text{-}NC}$	$X_{i\text{-}Control}$
I_1.Thermal performance	W/(mK)	DC_x	0.1	2.0	2.5	0.4	2.0	0.42	0.10	0.31
I_2.Acoustic performance	points	IC_v	0.0	0.5	0.3	0.9	1.1	0.15	0.20	0.08
I_3.Fire risk	%	DC_v	10.0	100.0	20.0	0.4	1.0	52	58	100
I_4 .Jobsite risk	points	DL	1.0	5.0	5.0	0.1	1.1	2.0	2.0	2.0
I_5.Visual quality	points	IL	1.0	10.0	10.0	0.1	1.0	7.0	7.0	7.0

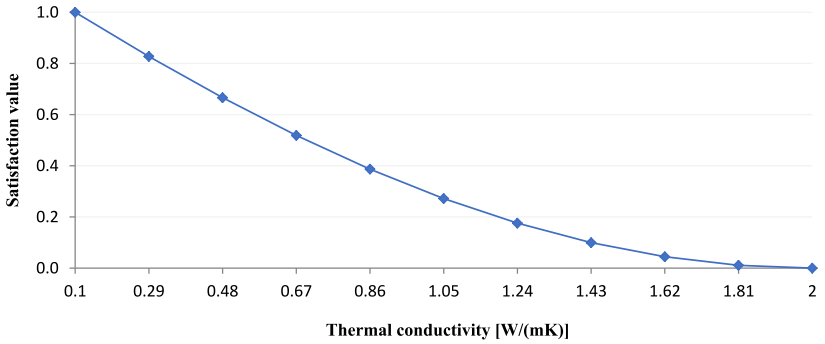

Fig. 11. Value function shape of indicator I_1.

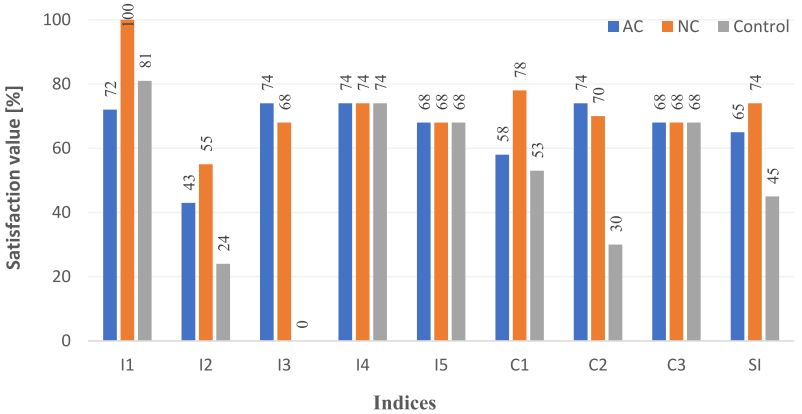

Fig. 12. Satisfaction values of all indices for the developed lime panels.

implementing the experimental results through the MIVES-based multi-objective approach, considering five indicators. The indicators and weights employed in this sustainability model can be easily adapted to other materials with similar functions while considering stakeholder and local sensitivities. The following outcomes may be reached from this study:

- Experimental characterization of insulation performance parameters revealed that the naturally cured lime composite (NC) displayed better performance than the accelerated cured composite (AC) in both thermal conductivity (up to 75%) and acoustic absorption (up to 35%) tests. Further, the NC composite showed superior properties than the control sample without fiber (up to 66% and 150% for thermal and acoustic tests) due to its lower density. However, both the NA and AC lime composite panels displayed acceptable performance as an insulator, as compared to other counterparts, thanks to the incorporation of the flax fabrics.
- The flexural strength of the accelerated carbonated composite (AC) was higher than that of the naturally carbonated one (NC) at all exposed temperatures (20 °C, 250 °C, and 450 °C). Indeed, in carbonated composites, calcite developed better, especially at low temperatures (as observed in XRD), leading to a denser and more interlocked microstructure, and ultimately, higher strength. Nevertheless, both lime composite panels presented higher flexural strength and energy absorption than the control sample, proving that the incorporation of nonwoven flax layers led to post-cracking behavior.

- Differences between the LOP (flexural resistance of the matrix) and MOR (maximum flexural resistance of the composite) values in both lime composites (AC and NC) decreased as the exposure temperature increased, suggesting a degradation of the flax reinforcement with temperature. Indeed, in both panels, fibers had no positive effect after 450 °C.
- As for the social sustainability assessment, both composite lime panels (especially the NC given the improved performance in thermal and acoustic tests) displayed a high satisfaction value (both above 65%) as compared to the panel without fiber, which was limited to 45%.

Thus, this study paved the way for further research aiming at enhancing the mechanical/durability performances and sustainability of natural textile-reinforced lime mortar composites. These results were yet preliminary and limited (namely in the scope of sustainability assessment); thus, further comprehensive analyses including tensile and durability performance of the lime panels, inclusive sustainability analysis by considering all three requirements of economic-environmental-social with more indicators, and the possibility of using the developed material as a strengthening system for masonry walls are being researched within the context of the Ph.D. thesis of the first author of this paper.

Declaration of competing interest

The authors declare that they have no known competing financial interests or personal relationships that could have appeared to influence the work reported in this paper.

Data availability

Data will be made available on request.

Acknowledgments

This work was supported through the project grants PID2019-108067RB-I00/AEI/10.13039/501100011033 and PID2020-117530RB-I00/MCIN/AEI/10.13039/501100011033 by the Ministerio de Ciencia e Innovación (MCIN)/Agencia Estatal de Investigación (AEI) of the Spanish Government. The author Payam Sadrolodabaee acknowledges the Banco Santander for the Research Scholarships (Postdoc-UPC 2022 Grant).

References

[1] P. Sadrolodabaee, J. Claramunt Blanes, M. Ardanuy Raso, A. de la Fuente Antequera, Preliminary study on new micro textile waste fiber reinforced cement composite, in: ICBBM 2021: 4th International Conference on Bio-Based Building Materials, 2021, pp. 37–42. Barcelona, Catalunya: June 16-18, https://upcommons.upc.edu/handle/2117/348199. (Accessed 22 July 2021) [Online]. Available:.
[2] C. Salzano, et al., Green building materials: mechanical performance and environmental sustainability, Mater. Sci. Forum 1082 (Mar. 2023) 296–301, https://doi.org/10.4028/P-C090IH.
[3] High energy performing buildings - publications Office of the EU. https://publications.europa.eu/en/publication-detail/-/publication/d8e3702d-c782-11e8-9424-01aa75ed71a1/language-en/format-PDF/source-77709912.
[4] I. Farina, I. Moccia, C. Salzano, N. Singh, P. Sadrolodabaee, F. Colangelo, Compressive and thermal properties of non-structural lightweight concrete containing industrial byproduct aggregates, Materials 15 (11) (Jun. 2022) 4029, https://doi.org/10.3390/MA15114029.
[5] S. Shahbazi, N. Singer, M. Majeed, M. Kavgic, R. Foruzanmehr, Cementitious insulated drywall panels reinforced with kraft-paper honeycomb structures, Buildings 12 (8) (Aug. 2022) 1261, https://doi.org/10.3390/BUILDINGS12081261.
[6] M. Ardanuy, J. Claramunt, R.D. Toledo Filho, Cellulosic fiber reinforced cement-based composites: a review of recent research, Construct. Build. Mater. 79 (2015) 115–128, https://doi.org/10.1016/j.conbuildmat.2015.01.035.
[7] P. Sadrolodabaee, J. Claramunt, M. Ardanuy, A. de la Fuente, A textile waste fiber-reinforced cement composite: comparison between short random fiber and textile reinforcement, Materials 14 (13) (Jul. 2021) 3742, https://doi.org/10.3390/MA14133742.
[8] E. Booya, K. Gorospe, H. Ghaednia, S. Das, Free and restrained plastic shrinkage of cementitious materials made of engineered kraft pulp fibres, Construct. Build. Mater. 212 (Jul. 2019) 236–246, https://doi.org/10.1016/J.CONBUILDMAT.2019.03.296.
[9] R.D. Toledo Filho, K. Ghavami, M.A. Sanjuán, G.L. England, Free, restrained and drying shrinkage of cement mortar composites reinforced with vegetable fibres, Cem. Concr. Compos. 27 (5) (2005) 537–546, https://doi.org/10.1016/j.cemconcomp.2004.09.005.
[10] P.J.M. Mehta, P.K, in: Montiero, Concrete Microstructure, Properties, and Materials, third ed., 2006. M.
[11] A.M. Brandt, Cement-Based Composites, CRC Press, 2005, https://doi.org/10.1201/9781482265866.
[12] P. Sadrolodabaee, J. Claramunt, M. Ardanuy, A. de la Fuente, Mechanical and durability characterization of a new textile waste micro-fiber reinforced cement composite for building applications, Case Stud. Constr. Mater. 14 (Jun. 2021), e00492, https://doi.org/10.1016/j.cscm.2021.e00492.
[13] M.P.M. Dicker, P.F. Duckworth, A.B. Baker, G. Francois, M.K. Hazzard, P.M. Weaver, Green composites: a review of material attributes and complementary applications, Compos Part A Appl Sci Manuf 56 (Jan. 2014) 280–289, https://doi.org/10.1016/J.COMPOSITESA.2013.10.014.
[14] P. Sadrolodabaee, Sustainability, durability and mechanical characterization of a new recycled textile-reinforced strain-hardening cementitious composite for building applications, UPC-BarcelonaTECH (2022). Doctoral Thesis, https://www.tdx.cat/handle/10803/674796.
[15] S. Spadea, I. Farina, A. Carrafiello, F. Fraternali, Recycled nylon fibers as cement mortar reinforcement, Construct. Build. Mater. 80 (Apr. 2015) 200–209, https://doi.org/10.1016/J.CONBUILDMAT.2015.01.075.
[16] H. Ventura, M.D. Álvarez, L. Gonzalez-Lopez, J. Claramunt, M. Ardanuy, Cement composite plates reinforced with nonwoven fabrics from technical textile waste fibres: mechanical and environmental assessment, J. Clean. Prod. 372 (Oct. 2022), 133652, https://doi.org/10.1016/J.JCLEPRO.2022.133652.
[17] P. Faria, F. Henriques, V. Rato, Comparative evaluation of lime mortars for architectural conservation, J. Cult. Herit. 9 (3) (2008) 338–346, https://doi.org/10.1016/j.culher.2008.03.003.
[18] D. Zhang, J. Zhao, D. Wang, C. Xu, M. Zhai, X. Ma, Comparative study on the properties of three hydraulic lime mortar systems: natural hydraulic lime mortar, cement-aerial lime-based mortar and slag-aerial lime-based mortar, Construct. Build. Mater. 186 (Oct. 2018) 42–52, https://doi.org/10.1016/J.CONBUILDMAT.2018.07.053.
[19] A.R. Mahpour, J. Claramunt, M. Ardanuy, J.R. Rosell, Flax Fabric-Reinforcement Lime Composite as a Strengthening System for Masonry Materials: Study of Adhesion, 2023, pp. 1297–1306, https://doi.org/10.1007/978-3-031-33211-1_116.
[20] R. Infante Gomes, C. Brazão Farinha, R. Veiga, J. de Brito, P. Faria, D. Bastos, CO2 sequestration by construction and demolition waste aggregates and effect on mortars and concrete performance - an overview, Renew. Sustain. Energy Rev. 152 (Dec. 2021), 111668, https://doi.org/10.1016/J.RSER.2021.111668.

[21] M. Arandigoyen, J.I. Alvarez, Pore structure and mechanical properties of cement–lime mortars, Cement Concr. Res. 37 (5) (May 2007) 767–775, https://doi.org/10.1016/J.CEMCONRES.2007.02.023.
[22] D. Ergenç, R. Fort, Accelerating carbonation in lime-based mortar in high CO2 environments, Construct. Build. Mater. 188 (Nov. 2018) 314–325, https://doi.org/10.1016/J.CONBUILDMAT.2018.08.125.
[23] G. Cultrone, E. Sebastián, M.O. Huertas, Forced and natural carbonation of lime-based mortars with and without additives: mineralogical and textural changes, Cement Concr. Res. 35 (12) (Dec. 2005) 2278–2289, https://doi.org/10.1016/J.CEMCONRES.2004.12.012.
[24] R.M. Dheilly, J. Tudo, Y. Sebaibi, M. Quéneudec, Influence of storage conditions on the carbonation of powdered Ca(OH)2, Construct. Build. Mater. 16 (3) (Apr. 2002) 155–161, https://doi.org/10.1016/S0950-0618(02)00012-0.
[25] B.A. Silva, A.P. Ferreira Pinto, A. Gomes, A. Candeias, Effects of natural and accelerated carbonation on the properties of lime-based materials, J. CO2 Util. 49 (December 2020) (2021), 101552, https://doi.org/10.1016/j.jcou.2021.101552.
[26] K. Van Balen, Carbonation reaction of lime, kinetics at ambient temperature, Cement Concr. Res. 35 (4) (Apr. 2005) 647–657, https://doi.org/10.1016/J.CEMCONRES.2004.06.020.
[27] D.T. Beruto, F. Barberis, R. Botter, Calcium carbonate binding mechanisms in the setting of calcium and calcium–magnesium putty-limes, J. Cult. Herit. 6 (3) (Jul. 2005) 253–260, https://doi.org/10.1016/J.CULHER.2005.06.003.
[28] G. Ferrara, M. Pepe, E. Martinelli, R.D. Tolêdo Filho, Tensile behavior of flax textile reinforced lime-mortar: influence of reinforcement amount and textile impregnation, Cem. Concr. Compos. 119 (May 2021), 103984, https://doi.org/10.1016/j.cemconcomp.2021.103984.
[29] G. Ferrara, M. Pepe, E. Martinelli, R.D.T. Filho, Influence of an impregnation treatment on the morphology and mechanical behaviour of flax yarns embedded in hydraulic lime mortar, Fibers 7 (4) (Apr. 2019) 30, https://doi.org/10.3390/FIB7040030.
[30] G. Ferrara, M. Pepe, R.D.T. Filho, E. Martinelli, Mechanical response and analysis of cracking process in hybrid TRM composites with flax textile and curauá fibres, Polymers 13 (5) (Feb. 2021) 715, https://doi.org/10.3390/POLYM13050715.
[31] C. Quintaliani, F. Merli, C.V. Fiorini, M. Corradi, E. Speranzini, C. Buratti, Vegetal fiber additives in mortars: experimental characterization of thermal and acoustic properties, Sustainability 14 (3) (Jan. 2022) 1260, https://doi.org/10.3390/SU14031260.
[32] O. Kinnane, A. Reilly, J. Grimes, S. Pavia, R. Walker, Acoustic absorption of hemp-lime construction, Construct. Build. Mater. 122 (Sep. 2016) 674–682, https://doi.org/10.1016/j.conbuildmat.2016.06.106.
[33] A. Rakhsh Mahpour, M. Ardanuy, H. Ventura, J.R. Rosell, J. Claramunt, Rheology, mechanical performance and penetrability through flax nonwoven fabrics of lime pastes, Construction Technologies and Architecture 1 (Jan. 2022) 480–490, https://doi.org/10.4028/WWW.SCIENTIFIC.NET/CTA.1.480.
[34] A. Rakhsh Mahpour, H. Ventura, M. Ardanuy, J.R. Rosell, J. Claramunt, The effect of fibres and carbonation conditions on the mechanical properties and microstructure of lime/flax composites, Cem. Concr. Compos. 138 (Apr. 2023), https://doi.org/10.1016/J.CEMCONCOMP.2023.104981.
[35] P. Sadrolodabaee, J. Claramunt, M. Ardanuy, A. de la Fuente, Effect of accelerated aging and silica fume addition on the mechanical and microstructural properties of hybrid textile waste-flax fabric-reinforced cement composites, Cem. Concr. Compos. 135 (Jan. 2023), 104829, https://doi.org/10.1016/J.CEMCONCOMP.2022.104829.
[36] P. Sadrolodabaee, J. Claramunt, M. Ardanuy, A. de la Fuente, Durability of eco-friendly strain-hardening cementitious composite incorporating recycled textile waste fiber and silica fume, in: *Fib Symposium*, 14th Fib PhD Symposium in Civil Engineering, fib. The International Federation for Structural Concrete, Rome, 2022, pp. 321–328 [Online]. Available: http://hdl.handle.net/2117/386845.
[37] J. Claramunt, L. Fernández-Carrasco, H. Ventura, M. Ardanuy, Natural fiber nonwoven reinforced cement composites as sustainable materials for building envelopes, Construct. Build. Mater. 115 (2016) 230–239, https://doi.org/10.1016/j.conbuildmat.2016.04.044.
[38] H. Ventura, M. Ardanuy, X. Capdevila, F. Cano, J.A. Tornero, Effects of needling parameters on some structural and physico-mechanical properties of needle-punched nonwovens, J. Textil. Inst. 105 (10) (2014) 1065–1075, https://doi.org/10.1080/00405000.2013.874628.
[39] L.M. do Amaral, C. de S. Rodrigues, F.S.J. Poggiali, Hornification on vegetable fibers to improve fiber-cement composites: a critical review, J. Build. Eng. 48 (May 2022), 103947, https://doi.org/10.1016/J.JOBE.2021.103947.
[40] P. Sadrolodabaee, J. Claramunt, M. Ardanuy, A. de la Fuente, Characterization of a textile waste nonwoven fabric reinforced cement composite for non-structural building components, Construct. Build. Mater. 276 (Mar. 2021), 122179, https://doi.org/10.1016/j.conbuildmat.2020.122179.
[41] G. Cultrone, E. Sebastián, M.O. Huertas, Forced and natural carbonation of lime-based mortars with and without additives: mineralogical and textural changes, Cement Concr. Res. 35 (12) (Dec. 2005) 2278–2289, https://doi.org/10.1016/J.CEMCONRES.2004.12.012.
[42] ASTM D5930." Standard Test Method for Thermal Conductivity by Means of a Transient Line-Source Technique.
[43] L. Gonzalez-Lopez, J. Claramunt, L. Haurie, H. Ventura, M. Ardanuy, Study of the fire and thermal behaviour of façade panels made of natural fibre-reinforced cement-based composites, Construct. Build. Mater. 302 (Oct. 2021), 124195, https://doi.org/10.1016/J.CONBUILDMAT.2021.124195.
[44] P. Sadrolodabaee, et al., Experimental characterization of comfort performance parameters and multi-criteria sustainability assessment of recycled textile-reinforced cement facade cladding, J. Clean. Prod. 356 (2022), https://doi.org/10.1016/j.jclepro.2022.131900.
[45] P. Sadrolodabaee, G. Di Rienzo, I. Farina, C. Salzano, N. Singh, F. Colangelo, Characterization of eco-friendly lightweight aggregate concretes incorporating industrial wastes, Key Eng. Mater. 944 (Apr. 2023) 209–217, https://doi.org/10.4028/p-s77l3k.
[46] ISO - ISO 10534-2:1998 - acoustics — determination of sound absorption coefficient and impedance in impedance tubes — Part 2: transfer-function method. https://www.iso.org/standard/22851.html. (Accessed 9 July 2021).
[47] R.M. Novais, et al., Multifunctional cork – alkali-activated fly ash composites: a sustainable material to enhance buildings' energy and acoustic performance, Energy Build. 210 (Mar. 2020), 109739, https://doi.org/10.1016/J.ENBUILD.2019.109739.
[48] Une 23725: 1990 Reaction to fire tests of materials. https://www.une.org/encuentra-tu-norma/busca-tu-norma/norma?c=N0002467. (Accessed 27 June 2021).
[49] R. Hay, C.P. Ostertag, Life cycle assessment (LCA) of double-skin façade (DSF) system with fiber-reinforced concrete for sustainable and energy-efficient buildings in the tropics, Build. Environ. 142 (Sep. 2018) 327–341, https://doi.org/10.1016/J.BUILDENV.2018.06.024.
[50] D. Kvočka, et al., Life cycle assessment of prefabricated geopolymeric façade cladding panels made from large fractions of recycled construction and demolition waste, Materials 13 (18) (2020), https://doi.org/10.3390/MA13183931.
[51] F. Colangelo, I. Farina, M. Travaglioni, C. Salzano, R. Cioffi, A. Petrillo, Eco-efficient industrial waste recycling for the manufacturing of fibre reinforced innovative geopolymer mortars: Integrated waste management and green product development through LCA, J. Clean. Prod. 312 (Aug. 2021), 127777, https://doi.org/10.1016/J.JCLEPRO.2021.127777.
[52] F. Lozano, J.C. Jurado, J.A. Lozano-Galant, A. de la Fuente, J. Turmo, Integration of BIM and value model for sustainability assessment for application in bridge projects, Autom. ConStruct. 152 (Aug. 2023), 104935, https://doi.org/10.1016/J.AUTCON.2023.104935.
[53] O. Pons, A. De La Fuente, J. Armengou, A. Aguado, Towards the sustainability in the design of wind towers, Energy Proc. 115 (Jun. 2017) 41–49, https://doi.org/10.1016/J.EGYPRO.2017.05.005.
[54] S. Hamed Banirazi Motlagh, S.M.A. Hosseini, O. Pons-Valladares, Integrated value model for sustainability assessment of residential solar energy systems towards minimizing urban air pollution in Tehran, Sol. Energy 249 (Jan. 2023) 40–66, https://doi.org/10.1016/J.SOLENER.2022.10.047.
[55] S.M.A. Hosseini, A. de la Fuente, O. Pons, Multicriteria decision-making method for sustainable site location of post-disaster temporary housing in urban areas, J. Construct. Eng. Manag. 142 (9) (2016), 04016036, https://doi.org/10.1061/(ASCE)CO.1943-7862.0001137.
[56] S.M.A. Hosseini, L. Farahzadi, O. Pons, Assessing the sustainability index of different post-disaster temporary housing unit configuration types, J. Build. Eng. 42 (Oct. 2021), 102806, https://doi.org/10.1016/J.JOBE.2021.102806.
[57] A. De La Fuente, O. Pons, A. Josa, A. Aguado, Multi-criteria decision making in the sustainability assessment of sewerage pipe systems, J. Clean. Prod. 112 (Jan. 2016) 4762–4770, https://doi.org/10.1016/j.jclepro.2015.07.002.
[58] O. Pons, Assessing the sustainability of prefabricated buildings, Eco-Efficient Construction and Building Materials: Life Cycle Assessment (LCA), Eco-Labelling and Case Studies (Jan. 2014) 434–456, https://doi.org/10.1533/9780857097729.3.434.

[59] J. Cuadrado, M. Zubizarreta, E. Roji, M. Larrauri, I. Alvarez, Sustainability assessment methodology for industrial buildings: three case studies 33 (2) (Apr. 2016) 106–124, https://doi.org/10.1080/10286608.2016.1148143.
[60] O. Pons, M.M. Casanovas-Rubio, J. Armengou, A. de la Fuente, Sustainability-driven decision-making model: case study of fiber-reinforced concrete foundation piles, J. Construct. Eng. Manag. 147 (10) (Oct. 2021), 04021116, https://doi.org/10.1061/(ASCE)CO.1943-7862.0002073/ASSET/DC634C63-48DE-47ED-8A12-E72CA499780E/ASSETS/IMAGES/LARGE/FIGURE6.JPG.
[61] G. Gilani, S.M.A. Hosseini, O. Pons-Valladares, A. de la Fuente, An enhanced multi-criteria decision-making approach oriented to sustainability analysis of building facades: a case study of Barcelona, J. Build. Eng. 54 (Aug. 2022), 104630, https://doi.org/10.1016/J.JOBE.2022.104630.
[62] F. Barrientos, et al., Knowledge-based minimization of railway infrastructures environmental impact, Transport. Res. Procedia 14 (Jan. 2016) 840–849, https://doi.org/10.1016/J.TRPRO.2016.05.032.
[63] A. de la Fuente, A. Blanco, J. Armengou, A. Aguado, Sustainability based-approach to determine the concrete type and reinforcement configuration of TBM tunnels linings. Case study: extension line to Barcelona Airport T1, Tunn. Undergr. Space Technol. 61 (Jan. 2017) 179–188, https://doi.org/10.1016/J.TUST.2016.10.008.
[64] O. Pons-Valladares, M. del M. Casanovas-Rubio, J. Armengou, A. de la Fuente, Approach for sustainability assessment for footbridge construction technologies: application to the first world D-shape 3D-Printed fiber-reinforced mortar footbridge in Madrid, J. Clean. Prod. 394 (Mar. 2023), 136369, https://doi.org/10.1016/J.JCLEPRO.2023.136369.
[65] P. Sadrolodabaee, et al., Experimental characterization of comfort performance parameters and multi-criteria sustainability assessment of recycled textile-reinforced cement facade cladding, J. Clean. Prod. 356 (Jul. 2022), 131900, https://doi.org/10.1016/J.JCLEPRO.2022.131900.
[66] P. Sadrolodabaee, S.M.A. Hosseini, M. Ardunay, J. Claramunt, A. de la Fuente, A New Sustainability Assessment Method for Façade Cladding Panels: A Case Study of Fiber/Textile Reinforced Cement Sheets, Sep. 2021, pp. 809–819, https://doi.org/10.1007/978-3-030-83719-8_69.
[67] G. Gilani, MCDM approach for assessing the sustainability of buildings' facades [Online]. Available: http://www.tdx.cat/?locale-.
[68] S.M.A. Hosseini, A. De, O. Pons, Multi-criteria decision-making method for assessing the sustainability of post-disaster temporary housing units technologies, A case study in Bam 20 (2016) 38–51, 2003.
[69] A. Aguado, A. del Caño, M.P. de la Cruz, D. Gómez, A. Josa, Sustainability assessment of concrete structures within the Spanish structural concrete code, J. Construct. Eng. Manag. 138 (2) (Feb. 2012) 268–276, https://doi.org/10.1061/(ASCE)CO.1943-7862.0000419.
[70] B. Alarcon, A. Aguado, R. Manga, A. Josa, A value function for assessing sustainability: application to industrial buildings, Sustainability 3 (1) (2011) 35–50, https://doi.org/10.3390/su3010035.
[71] I. Asadi, P. Shafigh, Z. F. bin Abu Hassan, and N. B. Mahyuddin, "Thermal conductivity of concrete – a review," J. Build. Eng., vol. 20, pp. 81–93, Nov. 2018, doi: 10.1016/J.JOBE.2018.07.002..
[72] P. Ricciardi, E. Belloni, F. Cotana, Innovative panels with recycled materials: thermal and acoustic performance and Life Cycle Assessment, Appl. Energy 134 (Dec. 2014) 150–162, https://doi.org/10.1016/J.APENERGY.2014.07.112.
[73] P. Bekhta, E. Dobrowolska, Thermal properties of wood-gypsum boards, Holz als Roh- Werkst. 64 (5) (Oct. 2006) 427–428, https://doi.org/10.1007/S00107-005-0074-8/METRICS.
[74] J. António, Acoustic behaviour of fibrous materials, in: Fibrous and Composite Materials for Civil Engineering Applications, Elsevier, 2011, pp. 306–324, https://doi.org/10.1533/9780857095583.3.306.
[75] R.M. Novais, L. Senff, J. Carvalheiras, A.M. Lacasta, I.R. Cantalapiedra, J.A. Labrincha, Simple and effective route to tailor the thermal, acoustic and hygrothermal properties of cork-containing waste derived inorganic polymer composites, J. Build. Eng. 42 (Oct. 2021), 102501, https://doi.org/10.1016/J.JOBE.2021.102501.
[76] T.S. Tie, K.H. Mo, A. Putra, S.C. Loo, U.J. Alengaram, T.C. Ling, Sound absorption performance of modified concrete: a review, J. Build. Eng. 30 (Jul. 2020), 101219, https://doi.org/10.1016/J.JOBE.2020.101219.
[77] P. Zhang, P. Zhang, J. Wu, Y. Zhang, J. Guo, Mechanical properties of polyvinyl alcohol fiber-reinforced cementitious composites after high-temperature exposure, Gels 8 (10) (Oct. 2022) 662, https://doi.org/10.3390/GELS8100662.
[78] E. Vejmelková, P. Konvalinka, P. Padevět, L. Kopecký, M. Keppert, R. Černý, Mechanical, hygric, and thermal properties of cement-based composite with hybrid fiber reinforcement subjected to high temperatures, Int. J. Thermophys. 30 (4) (Jun. 2009) 1310–1322, https://doi.org/10.1007/S10765-009-0609-Z.
[79] K.T.Q. Nguyen, S. Navaratnam, P. Mendis, K. Zhang, J. Barnett, H. Wang, Fire safety of composites in prefabricated buildings: from fibre reinforced polymer to textile reinforced concrete, Compos. B Eng. 187 (Apr. 2020), 107815, https://doi.org/10.1016/J.COMPOSITESB.2020.107815.
[80] M. Arandigoyen, B. Bicer-Simsir, J.I. Alvarez, D.A. Lange, Variation of microstructure with carbonation in lime and blended pastes, Appl. Surf. Sci. 252 (20) (Aug. 2006) 7562–7571, https://doi.org/10.1016/J.APSUSC.2005.09.007.
[81] D. Ergenç, L.S. Gómez-Villalba, R. Fort, Crystal development during carbonation of lime-based mortars in different environmental conditions, Mater. Char. 142 (Aug. 2018) 276–288, https://doi.org/10.1016/j.matchar.2018.05.043.
[82] M.D.M. Barbero-Barrera, O. Pombo, M.D.L.Á. Navacerrada, Textile fibre waste bindered with natural hydraulic lime, Compos. B Eng. 94 (Jun. 2016) 26–33, https://doi.org/10.1016/J.COMPOSITESB.2016.03.013.
[83] L. Gonzalez-Lopez, J. Claramunt, L. Haurie, H. Ventura, M. Ardanuy, Study of the fire and thermal behaviour of façade panels made of natural fibre-reinforced cement-based composites, Construct. Build. Mater. 302 (Oct. 2021), 124195, https://doi.org/10.1016/J.CONBUILDMAT.2021.124195.
[84] B. Georgali, P.E. Tsakiridis, Microstructure of fire-damaged concrete. A case study, Cem. Concr. Compos. 27 (2) (Feb. 2005) 255–259, https://doi.org/10.1016/J.CEMCONCOMP.2004.02.022.
[85] M. del Río Merino, J. Santa Cruz Astorqui, Finite element simulation to design constructive elements: an application to light gypsum plaster for partitions, Construct. Build. Mater. 23 (1) (Jan. 2009) 14–27, https://doi.org/10.1016/J.CONBUILDMAT.2007.12.009.
[86] A. Izaguirre, J. Lanas, J.I. Alvarez, Effect of a polypropylene fibre on the behaviour of aerial lime-based mortars, Construct. Build. Mater. 25 (2) (Feb. 2011) 992–1000, https://doi.org/10.1016/j.conbuildmat.2010.06.080.
[87] F. Iucolano, B. Liguori, C. Colella, Fibre-reinforced lime-based mortars: a possible resource for ancient masonry restoration, Construct. Build. Mater. 38 (2013) 785–789, https://doi.org/10.1016/j.conbuildmat.2012.09.050.
[88] L. Gonzalez-Lopez, J. Claramunt, Y. lo Hsieh, H. Ventura, M. Ardanuy, Surface modification of flax nonwovens for the development of sustainable, high performance, and durable calcium aluminate cement composites, Compos. B Eng. 191 (February) (2020), https://doi.org/10.1016/j.compositesb.2020.107955.
[89] J. Claramunt, H. Ventura, L.J. Fernández-Carrasco, M. Ardanuy, Tensile and flexural properties of cement composites reinforced with flax nonwoven fabrics, Materials 10 (2) (2017) 1–12, https://doi.org/10.3390/ma10020215.
[90] M. Frías Rojas, Study of hydrated phases present in a MK–lime system cured at 60 °C and 60 months of reaction, Cement Concr. Res. 36 (5) (May 2006) 827–831, https://doi.org/10.1016/J.CEMCONRES.2006.01.001.
[91] M. Martín-Garrido, S. Martínez-Ramírez, CO2 adsorption on calcium silicate hydrate gel synthesized by double decomposition method, J. Therm. Anal. Calorim. 143 (6) (Mar. 2021) 4331–4339, https://doi.org/10.1007/S10973-020-09374-8/METRICS.
[92] M.S. Morsy, A.F. Galal, S.A. Abo-El-Enein, Effect of temperature on phase composition and microstructure of artificial pozzolana-cement pastes containing burnt kaolinite clay, Cement Concr. Res. 28 (8) (Aug. 1998) 1157–1163, https://doi.org/10.1016/S0008-8846(98)00083-0.